JACS
JOURNAL OF THE AMERICAN CHEMICAL SOCIETY
Communication
pubs.acs.org/JACS

A Trigonal Prismatic Mononuclear Cobalt(II) Complex Showing Single-Molecule Magnet Behavior

Valentin V. Novikov,*[,†] Alexander A. Pavlov,[†] Yulia V. Nelyubina,[†] Marie-Emmanuelle Boulon,[‡] Oleg A. Varzatskii,[§] Yan Z. Voloshin,[†] and Richard E.P. Winpenny[‡]

[†]Nesmeyanov Institute of Organoelement Compounds, Russian Academy of Sciences, Moscow 119991, Russia
[‡]School of Chemistry and Photon Science Institute, The University of Manchester, Manchester M13 9PL, United Kingdom
[§]Vernadskii Institute of General and Inorganic Chemistry, The National Academy of Sciences of Ukraine, Kyiv 03680, Ukraine

Supporting Information

ABSTRACT: Single-molecule magnets (SMMs) with one transition-metal ion often rely on unusual geometry as a source of magnetically anisotropic ground state. Here we report a cobalt(II) cage complex with a trigonal prism geometry showing single ion magnet behavior with very high Orbach relaxation barrier of 152 cm^{-1}. This, to our knowledge, is the largest reported relaxation barrier for a cobalt-based mononuclear SMM. The trigonal prismatic coordination provided by the macrocyclic ligand gives intrinsically more stable molecular species than previously reported SMMs, thus making this type of cage complexes more amendable to possible functionalization that will boost their magnetic anisotropy even further.

Single-molecule magnets[1] (SMMs), the term referring to chemical compounds exhibiting slow magnetic relaxation and magnetic hysteresis of purely molecular origin,[2] were discovered in the early 1990's. Since then, they have emerged as perspective components for information storage,[3] quantum computing,[4] spintronics,[5] and magnetic refrigeration.[6,7] A necessary condition for a compound to be an SMM is a large axial magnetic anisotropy D that splits the energy levels of a metal ion under zero magnetic field and gives rise to an energy barrier between the states with opposite directions of the magnetic moment $U = |D|S^2$ (or, for non-integer S, $U = |D|(S^2 - 1/4)$). Although many polynuclear metal-containing clusters[1] and, more recently, lanthanide-,[8,9] actinide-,[10] and transition metal-based[11−13] mononuclear complexes have been reported to behave as SMMs,[14−16] their magnetic hysteresis occurred only at very low temperatures, making any successful technological applications infeasible.

Efforts toward systems with higher U were initially focused on achieving as large a total spin S[17] as possible; however, the magnetic anisotropy turned out to decrease with increasing S,[18] so the high value of U should be approached from the position of large $|D|$ value. This triggered a strong interest in mononuclear SMMs among many researchers. In contrast to rather complex polynuclear SMMs, which allowed obtaining very high S, mononuclear SMMs may be constructed with high $|D|$ by a more intuitive approach to rational molecular design.

A large magnetic anisotropy arises from a significant orbital contribution to the total magnetic moment. This contribution is a result of either an orbitally degenerate ground state with first-order orbital momentum unquenched by the crystal field,[19] or, if the orbital degeneracy is broken by a low-symmetry ligand field or a Jahn−Teller distortion, spin−orbit coupling (SOC) that reintroduces some orbital angular momentum into the ground state by mixing with a low-lying first excited state.[20] A smart choice of ligands may lead to a ground state of a compound that is degenerate, such as in the case of two-coordinate complexes of iron(I)[21] and iron(II)[22] with bulky ligands. These mononuclear complexes are linear and have a ground state with three electrons in the degenerate d_{xy} and $d_{x^2-y^2}$ orbitals; in the absence of any distortions, this should cause the orbital angular momentum of 2 μ_B to be added to the net spin moment.

Despite the impressive values of the relaxation barrier achieved to date for such transition-metal complexes (as high as 226 cm^{-1} for an iron(I) complex),[21] further improvement of their SMM properties is quite challenging: the linear geometry, which is a necessary condition for these compounds to be successful SMMs, may only be imposed by very bulky ligands, thus representing a severe limitation in the design of effective SMMs. On the other hand, a distortion of molecular geometry of a complex from linear, caused by vibronic effects or asymmetry of its ligands,[23] may not only reduce the D value but also result in a significant rhombic contribution to its magnetic anisotropy. The latter is, however, unfavorable for the SMM behavior, as it increases the rate of magnetization tunneling.[24] Therefore, a successful molecular design of transition-metal-based SMMs should pursue high overall symmetry of a mononuclear complex and at the same time keep dynamic distortions to a minimum.

A trigonal prism is a good choice for a coordination geometry that leads to a high negative value of D and possible SMM behavior in d^7 ions: trigonal prismatic cobalt(II) complexes have been recently found to demonstrate slow relaxation in a small[20] or even zero external static dc fields, with the largest barrier obtained[25] being 76 cm^{-1}. Very recently,[26] a large magnetic anisotropy ($D \approx -40$ cm^{-1}) was observed for a cobalt(II) cage complex (clathrochelate) **1**. Having the desired trigonal prismatic coordination geometry, clathrochelates exhibit tremendous rigidity of the chelating ligand, which prevents significant geometrical distortions[27] and ensures high chemical stability.[28] As most cobalt(II) clathrochelates are low spin at low

Received: June 3, 2015
Published: July 22, 2015

DOI: 10.1021/jacs.5b05739
J. Am. Chem. Soc. 2015, 137, 9792−9795

temperatures, no SMM behavior is expected for them owing to a large Jahn−Teller distortion that fully quenches their orbital moment.

We have recently reported a tris-pyrazoloximate ligand[29] that provides a ligand field sufficiently weak to make the resulting pseudo-clathrochelate transition-metal complexes high spin even at low temperatures. Among them, the cobalt(II) complex **2** (Figure 1a) showed a more than 2-fold increase in the values of

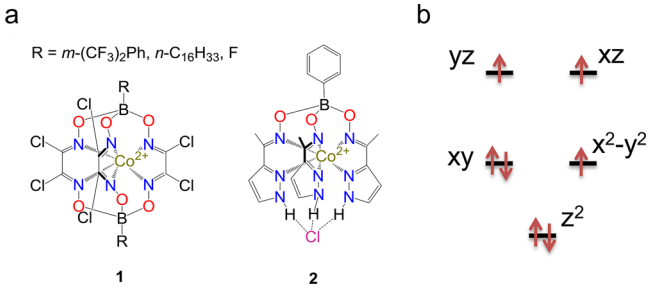

Figure 1. (a) Trigonal prismatic cage complexes with encapsulated cobalt(II) ion and (b) splitting of the d-orbitals for a perfect trigonal prism (only the configuration with doubly occupied *xy* orbital is shown).

pseudocontact shifts in NMR spectra in comparison with the boron-capped complexes **1**, which is also a sign of a significant increase in magnetic anisotropy.[30] Moreover, the orbital d_{z^2} in all the complexes **1** and **2** is nonbonding, and the qualitative d-orbital splitting pattern (Figure 1b) is the same as for the highly anisotropic d^7 iron(I) complex.[21] This suggests that **2** may be a very good SMM.

Variable-temperature dc magnetic susceptibility measurements show that the cobalt(II) ion in the complex **2** is high spin ($S = 3/2$) with a significant orbital contribution to the net magnetic moment (at 300 K, $\chi_M T$ is 2.87 cm^3 K mol^{-1}, Figure 2a); a gradual decrease in $\chi_M T$ with decreasing temperature

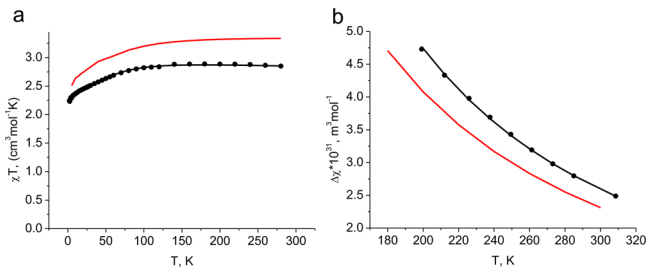

Figure 2. (a) Variable-temperature magnetic susceptibility data for a microcrystalline sample of **2** collected under an applied dc field of 1 kOe and (b) temperature dependence of magnetic susceptibility anisotropy obtained by NMR for a 3 mM solution of **2** in CD_2Cl_2. Black lines show fit to the data using eq 1, red lines represent the data from ab initio calculation obtained using the approach described in ref 35.

agrees with the presence of significant magnetic anisotropy.[22] Fitting the observed temperature dependence of magnetic susceptibility curves to spin Hamiltonian (eq 1):

$$\hat{H} = D\left(\hat{S}_z^2 - \frac{S(S+1)}{3}\right) + E(\hat{S}_x^2 - \hat{S}_y^2) + \mu_B g B \hat{S} \quad (1)$$

using the program *PHI*[31] results in the following magnetic parameters: $D = -82$ cm^{-1}, $E/D = 0.003$, $g_{\parallel} = 2.9$, $g_{\perp} = 2.2$. An acceptable fit is obtained only with the negative value of D and the axial g-tensor (see Supporting Information (SI) for more details). As the large D value prevents the population of excited states at low temperatures, the isofield magnetization curves (Supplementary Figure S1) are almost superimposable; although typically it implies the absence of magnetic anisotropy, a very large anisotropy (as shown for an isoelectronic iron(I) complex)[21] may also lead to the same result. Similar to a previously described cobalt(II)-based trigonal prismatic SMM,[20,25] no magnetic hysteresis was observed in variable-field magnetization data (Figure S2) at 2 K owing to quantum tunneling of magnetization (see below).

The sample is EPR silent at X- and Q-band frequencies in the temperature range 4−150 K, thus confirming the large negative value of D that gives rise to the ground state with $M_S = \pm 3/2$ and no observable intra-Kramers transitions.

Another way to obtain the values of D and g-tensor is to analyze NMR paramagnetic shifts. The pseudocontact shifts in the NMR spectra of **2** depend linearly on the axial anisotropy of magnetic susceptibility $\Delta\chi_{ax}$ (see SI for more details), which is given by the Van Vleck equation for a high-spin d^7 ion.[32] Fitting the temperature dependence of $\Delta\chi_{ax}$ from a variable-temperature NMR experiment (Figure 2b) by eq 1 gives the following parameters: $D = -109$ cm^{-1}, $g_{\parallel} = 2.9$, $g_{\perp} = 2.2$. They are close to those obtained from the dc magnetometry, especially considering that very different temperature ranges are covered and that the NMR study is performed in solution not solid state.

Although the results of dc magnetometry and NMR spectroscopy agree well, they are all based on a simple spin Hamiltonian eq 1, which may be inappropriate for a system with nearly degenerate orbitals and, therefore, large SOC.[19,33] For example, the isoelectronic Fe(I) complex[21] has the ground-state ^4E that is split by SOC into four doublets with the quantum numbers $M_J = \pm 7/2, \pm 5/2, \pm 3/2, \pm 1/2$. As this description, which is also applicable to the complex **2**, is quite different from the $M_S = \pm 3/2, \pm 1/2$ system described by the above spin Hamiltonian, the origins of its large magnetic anisotropy were assessed from multireference ab initio calculations using CASSCF/NEVPT2 approach implemented in ORCA software[34] (see SI for details). They give[35] a temperature dependence of both the magnetic susceptibility $\chi_M T$ and its anisotropy $\Delta\chi_{ax}$ (Figure 2) that agrees well with the experimental data, considering that for close-to-degenerate ground states, even the multireference calculations often fail to exactly reproduce magnetic features observed in the experiment.[35]

The computed phenomenological magnetic parameters in the zero magnetic field ($D = -110$ cm^{-1}, $E/D = 0.004$) are also very similar. As anticipated for a system with a degenerate ground state, the SOC splits the ground state into four doublets (Table S1); energy spacing between the two lowest doublets is, however, 220 cm^{-1} only, which is lower than the separation between the ground and the first excited states arising from an orbitally degenerate ground state, $2/3\zeta = 344$ cm^{-1} (ζ is the effective SOC constant, which is equal to 516 cm^{-1} for a free cobalt(II) ion).[36] This distinction suggests that the orbital momentum is partly quenched, possibly by a slight Jahn−Teller distortion[37] from a D_3 symmetry.[29] Although it seems that the large magnetic anisotropy of **2** results from the nearly degenerate ground state, the simple spin Hamiltonian eq 1 nevertheless provides an adequate approximation of the magnetic properties: as the second excited doublet is 840 cm^{-1} higher than the ground state, its population is below 1% even at room temperature. Thus, the observations from quantum chemistry confirm the presence of a very large magnetic anisotropy in **2**, as dc magnetometry and NMR spectroscopy do; if a simple equation $U = |D|(S^2 - 1/4)$ is

DOI: 10.1021/jacs.5b05739
J. Am. Chem. Soc. 2015, 137, 9792−9795

employed, one may expect the trigonal prismatic complex **2** to behave as an SMM with a very large value of magnetic reversal barrier ($2D$) of at least 164 cm^{-1}.

Ac magnetic susceptibility measurements were performed on microcrystalline samples of **2** to study the low-temperature relaxation dynamics for this compound. The plot of out-of-phase ac magnetic susceptibility χ''_M vs frequency has a maximum at 50 Hz (at 2 K), and its position is almost the same at 2−5 K but shifts to higher frequencies with further increase in the temperature (Figure 3a). Such a behavior is characteristic of

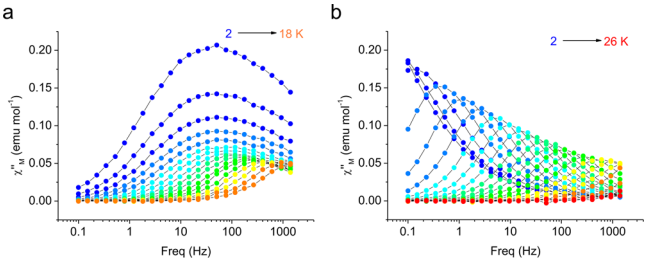

Figure 3. Out-of-phase χ''_M components of the ac magnetic susceptibility collected for a microcrystalline sample of **2** under (a) zero applied dc field and (b) applied dc field of 1.5 kOe. The corresponding in-phase χ'_M components of the ac magnetic susceptibility are shown in Figure S2.

quantum tunneling of magnetization (QTM) being the prevailing relaxation mechanism at low temperatures and then becoming less significant as thermal-activate relaxation processes dominate at higher temperatures. Although QTM is formally forbidden for complexes with odd electron count and axial magnetic anisotropy, hyperfine[38] or dipole−dipole[24] coupling may still result in a nonzero tunneling contribution.

Applying an external dc field at a constant temperature shifts the above maximum to lower frequencies (Figure S4); however, going beyond 1.5 kOe does not cause its additional shift. The out-of-phase susceptibility χ''_M has a maximum that is temperature dependent even at 2 K, thus implying the dramatically reduced probability of QTM in these conditions (Figure 3b). Fitting Cole−Cole plots[39] (Figure S5) using a generalized Debye model gives the temperature dependence of the relaxation time τ both in the zero field and in the external field of 1.5 kOe. As the Orbach (thermal) relaxation process results in an exponential temperature dependence of τ, its dominant contribution leads to linear Arrhenius plots ($\ln(\tau)$ vs $1/T$); however, both the Arrhenius plots (Figure 4) for the complex **2** are barely linear in the region of highest temperatures where the thermal relaxation is expected. If the linearity is assumed to hold in the temperature range 15−18 K, the U_{eff} values at zero and 1.5 kOe are then estimated as 71 and 101 cm^{-1}, respectively, which is very high for a mononuclear cobalt-based SMM. Such values, however, strongly contradict the above estimates of D, as no intermediate excited states are expected in this energy range.

Given that the parameters used for fitting the Cole−Cole plots (Tables S2−3) suggest the coexistence of multiple relaxation pathways, the relaxation data should be modeled with accounting for contributions from direct, QTM, Raman, and Orbach relaxation processes. Those are described by four consecutive terms in the following eq 2:

$$\tau^{-1} = AH^2T + \frac{B_1}{1 + B_2H^2} + CT^n + \tau_0^{-1}\exp(-U/kT) \quad (2)$$

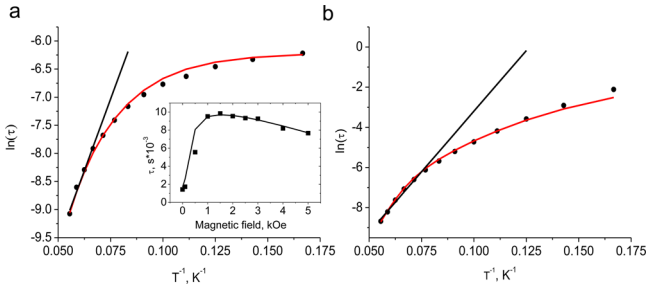

Figure 4. Arrhenius plots of the natural log of the relaxations time τ *vs* the inverse temperature, calculated from data at dc field of (a) 0 and (b) 1.5 kOe. Black lines show fit of the data in the range 15−18 K to the Arrhenius expression $\tau = \tau_0 \exp(U_{eff}/kT)$ using U_{eff} = 71 and 101 cm^{-1} for dc field of 0 and 1.5 kOe, respectively. Red lines show fit to the data using eq 2 with U = 152 cm^{-1}. Inset: Field dependence of the magnetic relaxation time, τ, at 10 K for a microcrystalline sample of **2** and its approximation by $\tau^{-1} = AH^2T + (B_1/(1 + B_2H^2)) + D$. Parameters A, B_1, and B_2 have the same meaning as in eq 2. The parameter D accounts for a nonzero contribution of the field-independent Raman and Orbach processes at 10 K. For other parameters of the fit, see Table S4.

where A, B_1, B_2, C, and n are coefficients, H is the magnetic field, T is the temperature, U is the thermal barrier of Orbach relaxation process, τ_0 is the attempt time, and k is the Boltzmann constant. Parameters related to direct and QTM relaxation mechanisms are determined from field-dependent ac magnetometry at 10 K (Figure S3), where only very small contributions from two-phonon Raman and Orbach processes are expected. Fitting of τ^{-1} vs H dependence by the first two terms of eq 2 allows obtaining values of A, B_1, and B_2 (Figure 4, inset). The position of the maximum at magnetic fields beyond 1.5 kOe is almost field-independent, which implies very small contribution of single phonon direct relaxation mechanism in contrast to many Fe(II) SMMs.[22] To further avoid overparametrization, the U value is considered to be the same at zero and 1.5 kOe, and the variable n related to the Raman process to be field-independent. Note that in the presence of other relaxation mechanisms, the attempt time τ_0 might have different values at various magnetic fields; thus, only five parameters (U and two sets of C and τ_0) are varied for simultaneous fitting of both zero and 1.5 kOe data. The best fits (Figure 4) irrespective of the initial values are obtained at n = 5 and U = 152 cm^{-1}; the latter closely matches the experimental $2D$ value of −164 cm^{-1}. Although the parameter n in the Raman relaxation pathway is usually equal to 9 for Kramers ions,[36] lower values may be expected if optical phonons are taken into account.[40−42] Relative contributions of three relaxation mechanisms vary significantly at zero and 1.5 kOe (Figure 5). The quantum tunneling relaxation, which only contributes in the zero field, dominates at low temperatures. In both the external fields of zero and 1.5 kOe, the Raman relaxation prevails at most temperatures, and the exponential Orbach pathway becomes important at the highest temperatures only. Nevertheless, the Raman process still influences greatly the overall relaxation properties, so the observed barrier of magnetization reversal (U_{eff} = 101 cm^{-1}) is far lower than the barrier of Orbach process only (U = 152 cm^{-1}).

Our theoretical and experimental data provide a consistent evidence of a trigonal cobalt(II) cage complex behaving as a single-molecule magnet with an extremely large thermal relaxation barrier. As recently pointed out by Zadrozny et al.,[22] even without quantum tunneling a very large first excitation energy does not necessarily result in a large magnetization

DOI: 10.1021/jacs.5b05739
J. Am. Chem. Soc. 2015, 137, 9792−9795

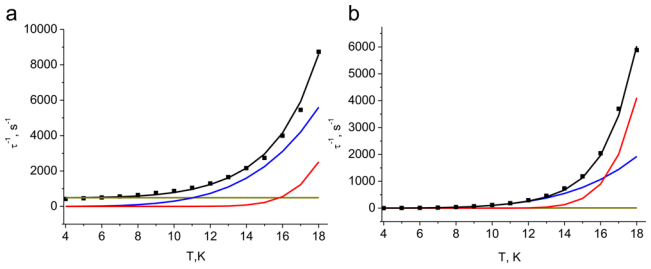

Figure 5. Temperature dependence of the inverse relaxation time $1/\tau$ calculated from data at dc field of (a) 0 and (b) 1.5 kOe. Black lines show fit to the data using eq 2 and parameters from Table S5; color lines show relative contributions of the possible relaxation pathways: direct and QTM (green), Orbach (red), and Raman (blue) processes.

reversal barrier, as a multiphonon Raman process may be more efficient in the absence of high-energy phonons. Therefore, any future optimization of SMM properties of cobalt(II) cage complexes (or other SMMs with an intrinsically large magnetic anisotropy) should address this important issue.

Large magnetic anisotropy of the reported compound follows from the same splitting of d-orbitals as in the record-holding iron(I) complex;[21] however, the trigonal prismatic coordination provided by the macrocyclic caging ligand gives intrinsically more stable molecular frameworks, thus making cage complexes more amendable to possible functionalization. Small changes in chelating fragments of the caging ligand may cause necessary changes in the ligand field and in the overall rigidity of a complex to boost the magnetic anisotropy even further while keeping the probability of undesirable relaxation pathways to a minimum; these studies are in progress in our group.

■ ASSOCIATED CONTENT

Supporting Information

The Supporting Information is available free of charge on the ACS Publications website at DOI: 10.1021/jacs.5b05739.

Experimental and computational details (PDF)

■ AUTHOR INFORMATION

Corresponding Author

*novikov84@ineos.ac.ru

Notes

The authors declare no competing financial interest.

■ ACKNOWLEDGMENTS

The study was supported by Russian Science Foundation (project 14-13-00724). B.M.E. and W.R.E.P. gratefully acknowledge support of the EPSRC(UK) (EP/L018470/1).

■ REFERENCES

(1) Sessoli, R.; Gatteschi, D.; Caneschi, A.; Novak, M. A. *Nature* **1993**, *365*, 141.

(2) Gatteschi, D.; Sessoli, R.; Villain, J. *Molecular Nanomagnets*; Oxford University Press: Oxford, U.K., 2006.

(3) Mannini, M.; Pineider, F.; Sainctavit, P.; Danieli, C.; Otero, E.; Sciancalepore, C.; Talarico, A. M.; Arrio, M.-A.; Cornia, A.; Gatteschi, D. *Nat. Mater.* **2009**, *8*, 194.

(4) Winpenny, R. E. *Angew. Chem., Int. Ed.* **2008**, *47*, 7992.

(5) Bogani, L.; Wernsdorfer, W. *Nat. Mater.* **2008**, *7*, 179.

(6) Karotsis, G.; Kennedy, S.; Teat, S. J.; Beavers, C. M.; Fowler, D. A.; Morales, J. J.; Evangelisti, M.; Dalgarno, S. J.; Brechin, E. K. *J. Am. Chem. Soc.* **2010**, *132*, 12983.

(7) Peng, J.-B.; Zhang, Q.-C.; Kong, X.-J.; Zheng, Y.-Z.; Ren, Y.-P.; Long, L.-S.; Huang, R.-B.; Zheng, L.-S.; Zheng, Z. *J. Am. Chem. Soc.* **2012**, *134*, 3314.

(8) Sessoli, R.; Powell, A. K. *Coord. Chem. Rev.* **2009**, *253*, 2328.

(9) Ishikawa, N.; Sugita, M.; Ishikawa, T.; Koshihara, S.-y.; Kaizu, Y. *J. Am. Chem. Soc.* **2003**, *125*, 8694.

(10) Meihaus, K. R.; Long, J. R. *Dalton Trans.* **2015**, *44*, 2517.

(11) Freedman, D. E.; Harman, W. H.; Harris, T. D.; Long, G. J.; Chang, C. J.; Long, J. R. *J. Am. Chem. Soc.* **2010**, *132*, 1224.

(12) Harman, W. H.; Harris, T. D.; Freedman, D. E.; Fong, H.; Chang, A.; Rinehart, J. D.; Ozarowski, A.; Sougrati, M. T.; Grandjean, F.; Long, G. J. *J. Am. Chem. Soc.* **2010**, *132*, 18115.

(13) Craig, G. A.; Murrie, M. *Chem. Soc. Rev.* **2015**, *44*, 2135.

(14) Layfield, R. A. *Organometallics* **2014**, *33*, 1084.

(15) Woodruff, D. N.; Winpenny, R. E.; Layfield, R. A. *Chem. Rev.* **2013**, *113*, 5110.

(16) Feltham, H. L.; Brooker, S. *Coord. Chem. Rev.* **2014**, *276*, 1.

(17) Ako, A. M.; Hewitt, I. J.; Mereacre, V.; Clérac, R.; Wernsdorfer, W.; Anson, C. E.; Powell, A. K. *Angew. Chem.* **2006**, *118*, 5048.

(18) Neese, F.; Pantazis, D. A. *Faraday Discuss.* **2011**, *148*, 229.

(19) Palii, A.; Clemente-Juan, J.; Coronado, E.; Klokishner, S.; Ostrovsky, S.; Reu, O. *Inorg. Chem.* **2010**, *49*, 8073.

(20) Gomez-Coca, S.; Cremades, E.; Aliaga-Alcalde, N.; Ruiz, E. *J. Am. Chem. Soc.* **2013**, *135*, 7010.

(21) Zadrozny, J. M.; Xiao, D. J.; Atanasov, M.; Long, G. J.; Grandjean, F.; Neese, F.; Long, J. R. *Nat. Chem.* **2013**, *5*, 577.

(22) Zadrozny, J. M.; Atanasov, M.; Bryan, A. M.; Lin, C. Y.; Rekken, B. D.; Power, P. P.; Neese, F.; Long, J. R. *Chem. Sci.* **2013**, *4*, 125.

(23) Atanasov, M.; Zadrozny, J. M.; Long, J. R.; Neese, F. *Chem. Sci.* **2013**, *4*, 139.

(24) Gatteschi, D.; Sessoli, R. *Angew. Chem., Int. Ed.* **2003**, *42*, 268.

(25) Zhu, Y.-Y.; Cui, C.; Zhang, Y.-Q.; Jia, J.-H.; Guo, X.; Gao, C.; Qian, K.; Jiang, S.-D.; Wang, B.-W.; Wang, Z.-M. *Chem. Sci.* **2013**, *4*, 1802.

(26) Novikov, V. V.; Pavlov, A. A.; Belov, A. S.; Vologzhanina, A. V.; Savitsky, A.; Voloshin, Y. Z. *J. Phys. Chem. Lett.* **2014**, *5*, 3799.

(27) Novikov, V. V.; Ananyev, I. V.; Pavlov, A. A.; Fedin, M. V.; Lyssenko, K. A.; Voloshin, Y. Z. *J. Phys. Chem. Lett.* **2014**, *5*, 496.

(28) Voloshin, Y. Z.; Varzatskii, O. A.; Vorontsov, I. I.; Antipin, M. Y. *Angew. Chem., Int. Ed.* **2005**, *44*, 3400.

(29) Varzatskii, O. A.; Penkova, L. V.; Kats, S. V.; Dolganov, A. V.; Vologzhanina, A. V.; Pavlov, A. A.; Novikov, V. V.; Bogomyakov, A. S.; Nemykin, V. N.; Voloshin, Y. Z. *Inorg. Chem.* **2014**, *53*, 3062.

(30) Damjanovic, M.; Katoh, K.; Yamashita, M.; Enders, M. *J. Am. Chem. Soc.* **2013**, *135*, 14349.

(31) Chilton, N. F.; Anderson, R. P.; Turner, L. D.; Soncini, A.; Murray, K. S. *J. Comput. Chem.* **2013**, *34*, 1164.

(32) Kahn, O. *Molecular magnetism*; Wiley-VCH, Inc.: New York, 1993.

(33) McGarvey, B. R.; Telser, J. *Inorg. Chem.* **2012**, *51*, 6000.

(34) Neese, F. *Wiley Interdisciplinary Reviews: Computational Molecular Science* **2012**, *2*, 73.

(35) Atanasov, M.; Ganyushin, D.; Pantazis, D. A.; Sivalingam, K.; Neese, F. *Inorg. Chem.* **2011**, *50*, 7460.

(36) Abragam, A.; Bleaney, B. *Electron paramagnetic resonance of transition ions*; Oxford University Press: Oxford, U.K., 2012.

(37) Ruamps, R.; Maurice, R.; Batchelor, L.; Boggio-Pasqua, M.; Guillot, R.; Barra, A. L.; Liu, J.; Bendeif, E.; Pillet, S.; Hill, S. *J. Am. Chem. Soc.* **2013**, *135*, 3017.

(38) Gómez-Coca, S.; Urtizberea, A.; Cremades, E.; Alonso, P. J.; Camón, A.; Ruiz, E.; Luis, F. *Nat. Commun.* **2014**, *5*, 4300.

(39) Cole, K. S.; Cole, R. H. *J. Chem. Phys.* **1941**, *9*, 341.

(40) Shrivastava, K. *Phys. Status Solidi B* **1983**, *117*, 437.

(41) Colacio, E.; Ruiz, J.; Ruiz, E.; Cremades, E.; Krzystek, J.; Carretta, S.; Cano, J.; Guidi, T.; Wernsdorfer, W.; Brechin, E. K. *Angew. Chem., Int. Ed.* **2013**, *52*, 9130.

(42) Singh, A.; Shrivastava, K. *Phys. Status Solidi B* **1979**, *95*, 273.

DOI: 10.1021/jacs.5b05739
J. Am. Chem. Soc. 2015, 137, 9792−9795